Research Square

Preprints are preliminary reports that have not undergone peer review.
They should not be considered conclusive, used to inform clinical practice,
or referenced by the media as validated information.

Buccitoxins and muritoxins: Conotoxin-like peptides in non-conoidean venoms revealed with a novel bioassay

Luke Levensaler

lukelevensaler@gmail.com

Kimball Union Academy

Article

Keywords:

Posted Date: November 3rd, 2026

DOI: https://doi.org/10.21203/rs.3.rs-10988105/v1

License: This work is licensed under a Creative Commons Attribution 4.0 International License.
Read Full License

Additional Declarations: No competing interests reported.

Buccitoxins and muritoxins: Conotoxin-like peptides in non-conoidean venoms revealed with a novel bioassay

Luke Levensaler (lukelevensaler@gmail.com)

ABSTRACT

Salivary venom samples were obtained from the radular glands of Lightning Whelk (Sinistrofulgur perversum), Apple Murex (Phyllonotus pomum), and Pear Whelk (Fulguropsis spirata) specimens. Extraction was performed via pressure application to the mid-esophageal and accessory salivary glands. The Apple Murex belongs to the superfamily Muricoidea, while the Lightning and Pear Whelks belong to Buccinoidea. It was hypothesized that the overall structural characteristics of their venomic peptidomes would mirror those of conotoxins. Peptidomes extracted via $(NH)_2SO_4$ precipitation were preprocessed by centrifugation and analyzed using the novel Levensaler Immobilized Metal Chelate Affinity Labelling Assay (LIMCALA). This assay was specifically designed for high-level Neogastropod venomic analyses in field environments, such as research vessels, where HPLC-MS is impractical. The resulting data, processed through the Levensaler Neogastropod Venomic Similarity Indexing (LNVSI) machine-learning algorithm, yielded high, statistically significant composite similarity scores against an α-conotoxin VxXXC positive control. These findings strongly suggest the presence of buccinoidean and muricoidean conotoxin-like myotoxins, termed “buccitoxins” and “muritoxins”, warranting further investigation into their pharmacological potential.

INTRODUCTION

Since the 1970s, the scientific community has made great strides in the field of marine pharmaceuticals. Many innovative possible treatments–originating from the biodiversity of ocean life–have been discovered for some of humanity's most pressing medical problems (National Research Council Committee on the Ocean's Role in Human Health, 1999). Among the many marine organisms at the center of these biomedical findings, cone snails are undoubtedly the most well-known across popular culture, marine biology, and medicine. These mollusks are carnivorous, predatory, harpoon-hunting sea snails belonging to the family Conidae that usually inhabit the benthic ecosystems of temperate and tropical neritic waters from the subtidal zone down to 100 m deep and sometimes deeper, killing small prey with their immobilizing, cardiac arrest-inducing complex venoms (Kohn & Perron, 1994, as cited in Cunha et al., 2014). The discovery in 1978 of the diverse and highly specific bioactive properties of peptides found within the venoms of cone snails has opened up a whole new area of cutting-edge pharmaceutical research (Li et al., 2020). These myotoxins (animal venom peptides) are called "conotoxins" (or conopeptides) and have been classified into a variety of pharmacological groups with different properties determined by Cysteine (Cys) arrangement patterns, or "frameworks", and genetic superfamilies. Such properties are potentially valuable for the creation of advanced, safer, and more effective non-opioid analgesics, ultra-specific and effective cancer treatments (in the case of α-conotoxins, especially), and antidepressant medications (Urani et al., 2002; Robinson & Norton, 2014).

Recent breakthrough research found that potentially biomedically useful peptides may not exist within only Conidae venomic proteomes, or even just Conoidean proteomes. Aside

from harpoon-hunting cone snails, several neogastropod taxa with chitinous radular teeth also produce venoms containing cysteine-rich small peptides. These include the conoidean families Turridae and Terebridae, as well as *Vexillum*, a non-conoidean genus in the family Costellariidae (superfamily Turbinelloidea) (Gorson et al., 2015; Hernández-Sámano et al., 2020; Kuznetsova et al., 2022). Some "teretoxins" derived from terebras, like the Subulate Auger (*Terebra subulata*), have been found to have XIV Cys frameworks, which, in cone snails, are usually associated with α-conotoxin pharmacological behavior (Gao et al., 2017; Gorson et al., 2015, as cited in Peng et al., 2006; Kendel et al., 2013).

Whelks and murexes belong to the superfamilies Buccinoidea and Muricoidea, respectively, within the order Neogastropoda. These taxa inhabit a variety of benthic habitats all over the world, from the intertidal zone down to the bathyal zone, 1,000 to 4,000 m below the ocean surface (Barco et al., 2010; Vaux et al., 2017). Although they can be either predators or scavengers, many are strictly predatory and feed using a specialized radula. Instead of delivering venom via a chitinous tooth (like the toxoglossate Turridae and Terebridae) or a hypodermic harpoon (Conidae) found in other conoideans, these snails introduce toxins through their saliva, similar to the envenomation mechanics of terrestrial Gila monsters (*Heloderma suspectum*) and northern short-tailed shrews (*Blarina brevicauda*).

Little is currently known about the proteomes of the salivary venoms produced by non-Conoidean neogastropods, commonly known as murexes and whelks. However, many studies featuring the salivary venom of the dog whelk (*Nucella lapillus*)[1] seem to suggest that

[1] The Dog Whelk (*Nucella lapilius*) is not a true Buccinid whelk and actually belongs to Muricidae.

“muritoxins” and “buccitoxins” may exist. These whelk and murex myotoxins may share Cys structure frameworks and pharmacological behavior in common with conotoxins of high biomedical potential, such as α-conotoxins (Martoja, 1971; Andrews, 1991; Andrews et al, 1991). Transcriptomic evidence of conotoxin-like mRNA sequences has also been found in the muricoidean veined rapa whelk (*Rapana venosa*) and the buccinoidean *Hemifusus tuba* (Song et. al, 2016; Li et. al, 2019). Additionally, a landmark study conducted in cooperation with various universities in Spain and Italy identified true putative conotoxin-like genes in the transcriptomes of the muricoidean *Stramonita haemastoma*. The research used “shotgun” proteomics to cross-reference these DNA exon sequences to actual expressed venomic peptides identified via ultra-precise High-Performance Liquid Chromatography with Mass Spectroscopy (HPLC-MS) and the DeTox software algorithm (Ringeval et. al, 2026). These cone snail-*S. haemastroma* ohnologs were not recognized as novel muritoxins because automated bioinformatics pipelines like DeTox rely strictly on pre-existing FASTA databases. If such Cys-rich myotoxins physically and structurally exist in whelk and murex venoms, they would be a highly promising area of study within the field of bioprospecting and marine-derived pharmaceuticals.

Consequently, in this research, salivary venoms from the buccinoidean lightning whelk (*Sinistrofulgur perversum*), pear whelk (*Fulguropsis spirata*), and the muricoidean apple murex (*Phyllonotus pomum*) were collected and analyzed for structural similarity to a known conotoxin positive control: α-conotoxin VxXXC. Each peptidome sample was subjected to the novel Levensaler Immobilized Metal Chelate Affinity Labelling Assay (LIMCALA), a technique designed to amplify the spectral resonances of key cysteine (Cys) features across proteins. This assay integrates conceptual elements from both Enzyme-Linked Immunosorbent Assay (ELISA)

and Immobilized Metal Chelate Affinity Chromatography (IMCAC), enabling detailed spectral data acquisition across the ultraviolet-A (UVA), visible, and near-infrared (NIR) ranges.

The resulting data provides a comprehensive peptidomic profile for each sample. These profiles were then analyzed using the Levensaler Neogastropod Venomic Similarity Indexer (LNVSI) algorithm, which quantitatively compares each sample's spectral features to those of the conotoxin positive control. Statistically significant similarity scores indicate meaningful Cys-driven primary structure overlap between the analyzed neogastropod venom peptides and established conotoxins.

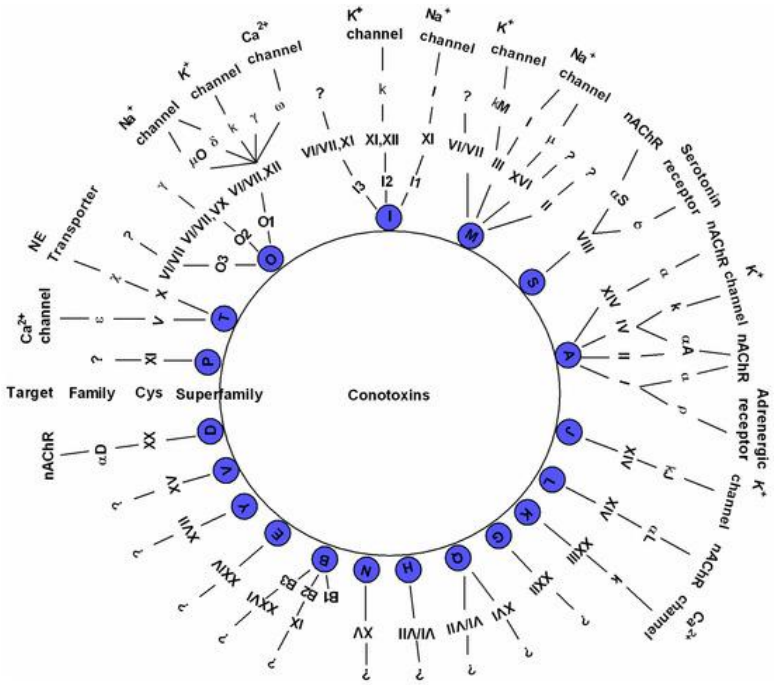
High similarity scores suggest that the myotoxins from these three buccinoidean and muricoidean species may represent true buccitoxins and muritoxins, respectively. In particular, especially high continuity with the α-conotoxin VxXXC control may imply shared cysteine frameworks, an especially promising indicator of therapeutic potential in anticancer research.

BACKGROUND

Cone snail venom owes its, albeit theoretical, biomedical versatility to its diverse set of peptide and protein components. Each of these macromolecular components performs a different function in these snails' venomic proteomes, and they are categorized by pharmacological class, with different Greek letters assigned to groups of peptides that interact with various animal cells differently (Gao et al., 2017). Most conotoxins are small, usually 10-35 amino acids in length, and usually have few additional post-translational features (Buczek et al., 2005). While there is usually a connection between pharmacological class and the Roman letter-demarcated genetic superfamilies of the transcribed exon loci responsible for producing these peptides, some conotoxins are part of the same pharmacological class and behave very similarly at a

biochemical level, but come from different genetic superfamilies (Robinson & Norton, 2014). Conotoxins are also categorized by their structural Cysteine (Cys) frameworks, which are differentiated from each other by Roman numerals. These Cys frameworks represent the linear arrangement of the Cys residues in a peptide's primary structure.

Figure 1



The diagram illustrates the relationship between conotoxin genes, structural Cys frameworks, pharmacological classes, and cell membrane targets, with each level serving as a determiner of the next in that order (Gao et al., 2017).

Not all components of cone snail venoms fit into the aforementioned genetic and peptidomic categorization system, however. Many species' venomic proteomies also contain larger-mass conoproteins, con ikot-ikots, conoCAPs, conopressins, conodipines, and

conkunitzins. Con ikot-ikots desensitize AMPA-type glutamate receptors, conoCAPs have been shown to effectively reduce blood pressure and heart rate in laboratory mice, conopressins inhibit vasopressin receptors, and conokunitzins inhibit K^+ transport channels (Robinson & Norton, 2014; Möller et al., 2019).

Of all the components of cone snail venom, the α-conotoxin pharmacological family is a highly medically interesting group of bioactive macromolecules. These peptides have exhibited inhibitory effects on Nicotinic Acetylcholine Receptors (nAChR) in numerous studies, which have been documented to result indirectly in anticancer properties. Such impacts on cancer cell survival have been characterized by this literature as being selectively cytotoxic and versatile, ranging from anti-angiogenesis properties to metastasis inhibition, as well as direct capability to trigger apoptosis. (Abraham et al., 2017; Osipov et al., 2020). As such, many across the public and the scientific community have hypothesized about the potential of these peptides to be exploited in the pharmaceutical development of a hypothetical highly-selective "magic bullet" treatment for cancer.

Designing and producing a new pharmacological therapeutic regimen from a conotoxin is a complicated task that takes years of effort and proper funding. Many have failed at it due to biochemical and logistical reasons. However, it has been done successfully before with the creation of Prialt® (ziconotide). Ziconotide is an analog of the ω-conotoxins GVIA from Geography Cone (*Conus geographus*) and MVIIA from the Magician's Cone (*Conus magus*), which were discovered at the University of Utah (Safavi-Hemami et al., 2019). It is the first and, so far, the only, FDA approved non-opioid intrathecal infusion treatment for severe pain. The research efforts were spearheaded by Dr. Baldomero Olivera, who also helped to discover the

first known conopeptide from *Conus geographus* in 1978. The United States Federal Drug Administration approved Prialt® for intrathecal use in 2004. (Cruz et al., 1978; Safavi-Hemami et al., 2019).

The family Conidae belongs to the order Neogastropoda. The complex venomic peptidomes of the many species representing Conidae have shown potential for revolutionizing many fields of medicine. However, some studies conducted within the last twenty years have revealed the existence of peptides similar to conotoxins within Neogastropoda, but in the venoms of taxa outside of Conidae. Neogastropoda are carnivorous, predatory, or scavenger aquatic and marine snails, and there are many venomous, non-Conidae sea snails within this taxon. For example, *Triplostephanus anilis* and the Chocolate Spotted Auger (*Terebra subulata*), two species of the family Terebridae, have been found to contain disulfide and Cys-based peptides very similar to conotoxins in primary structure and composition, yet divergent in secondary structure that have come to be known to marine biologists as "teretoxins" in their venomic proteomes (Gorson et al., 2015, as cited in Imperial et al., 2007; Anand et al., 2014). Some of these teretoxins have been found both to share the Cys frameworks of XIV conotoxins and to have similar nAChR-inhibiting properties to α-conotoxins (Gorson et al., 2015, as cited in Peng et al., 2006; Kendel et al., 2013). The Noble Giant Turrid (*Polystira nobilis*), a member of Turridae, another Neogastropod family, has also been determined to possess its own highly specific bioactive peptides similar to conotoxins. These myotoxins are referred to in the limited literature on turrid venomic biology as "turritoxins" (Hernández-Sámano et al., 2020). Like the XIV teretoxins, some of these turritoxins have also displayed nAChR-inhibiting properties that could, theoretically, like α-conotoxins, be useful for creating effective anticancer pharmaceuticals (Hernández-Sámano et al., 2020).

Turrids and terebras are the taxonomic neighbors of cone snails, within the superfamily Conoidea. Venomic composition and biochemical continuity between taxa are often predicated on evolutionary proximity when it comes to predatory sea snails, because Neogastropod myotoxin synthesis is closely related to phylogenetics (Cunha et al., 2014a; Robinson & Norton, 2014b). Thus, it is currently mostly unclear to the scientific community what myotoxins may be present in predatory non-Conoidean venoms and how they will structurally and pharmacologically compare to those of cone snails. It is also unknown how the venom components of such snails behave at a cellular level when introduced to living tissues and how such biochemical behavior could be utilized in pharmaceuticals, especially the seemingly promising nAChR inhibition anticancer drugs. The only real insight marine biologists and biochemists have into the venom components of these invertebrates is a recent (at the time of writing) study that confirmed the existence of Cys-rich bioactive peptides in the venoms of the *Vexillum* genus called "vexitoxins" (Kuznetsova et al., 2022).[2] Some vexitoxins were found to have similar Cys frameworks and compositions to many specific conotoxins, including α-conotoxins and other nAchR-inhibiting conotoxins from other pharmacological groups, showing promise for worthwhile further biomedical research on non-Conoidean myotoxins and venomic proteomes (Robinson & Norton, 2014; Kuznetsova et al., 2022). The body of scientific knowledge on the peptidomes of non-Conoidean Neogastropod marine snails is lacking in depth and scope, even more so than the topic of non-cone snail Conoidean venomics. However, the

[2] This genus is part of the Costellaridae, a family of small predatory sea snails known as a type of "micromollusc" living in tropical benthic ecosystems from the intertidal zone to 200m deep (Fedosov et al., 2017).

substantial body of promising discoveries from cone snail venomics research suggests that non-Conoidean venomics likewise holds significant potential for biomedical applications.

METHODS

Salivary Venom Extraction and Procurement

Populations of individual snails belonging to the three species from which salivary venom was collected were kept in species-segregated tanks throughout the course of the experiment. These species of marine Neogastropod snails included the buccinoidean Lightning Whelks (*Sinistrofulgur perversum*), Pear Whelks (*Fulguropsis spirata*), and the muricoidean Apple Murexes (*Phyllonotus pomum*). Their environments consisted of 3 species-segregated 5-gallon glass seawater tanks heated to 25°C, aerated, and containing filtration systems. Their sunlight photoperiods were maintained naturally through exposure to ambient daylight from glass windows as the primary light source, although laboratory lighting may have introduced minor disruptions. Thus, they were kept in sync with the December through January day/night cycle for the location of the laboratory, on Hilton Head Island, South Carolina. The snails were fed every 3-5 days, depending on their rejection or acceptance of their food items, strictly using fresh local Northern Quahog meat (*Mercenaria mercenaria*) meat from local seafood vendors on Hilton Head. Their salivary venoms were harvested as needed via dissection. To begin, each harvested individual was placed in a 2.5 cm deep aerated seawater preparation, where the waterline fully submerged the shell opening and foot. There, the snail was given a piece of Northern Quahog meat and allowed to begin feeding on it, before being swiftly removed from the tank and placed on a dissection tray. The shell aperture was then removed promptly with pliers, as well as its operculum. Such preparation was done with the goal of triggering the snail

to produce fresh and proteomically diverse saliva in anticipation of feeding. A longitudinal cut was then made down the cephalic foot, from between the eyestalks to its base. The radular proboscis stalk was, in the process, bisected to reveal the associated mid-esophageal and accessory salivary glands. Pressure was applied using forceps at the location of the salivary glands, allowing the venom to seep out and be extracted using a 10 mL single-use plastic syringe. These samples were then collected in labelled species-segregated vials, which were then centrifuged at 10,000 x g for 2 minutes to remove any cellular material, mucin, which is composed of glycoproteins, or microbes. The venom samples, which were contained in the aqueous supernatants and consisted of the venoms of all the harvested species-specific tank individuals, were carefully micropipetted into 250 µL cryovial aliquots. 250 µL of glycerol was added to each of these aliquots for peptide stability during their storage at -20°C in a low-temperature consumer freezer to prevent denaturation, creating a 50% glycerol, 50% snail venom long-term storage stock solution with a volume of 0.5 mL. When these venom stock solutions were ready to be used in the following LIMCALA procedures, they were thawed at 4°C in the IVYX Scientific 5L Incubator, and 0.5 mL of deionized (DI) water was added to their aliquots. That freezer and the IVYX Scientific 5L Incubator were consistently used throughout this entire study to keep reagents and samples at, respectively, -20°C and 4°C. The water added was the solvent for the 1M Ammonium Sulfate $(NH_4)_2SO_4$ solutions created in the aliquots for the purpose of "salting out" their pure peptidomic samples via precipitation. The aliquots were then agitated via another round of centrifugation at 10,000 x g for 2 minutes to cleanly separate the purely proteomic precipitate as a pellet from the remaining and discarded non-proteomic supernatant solution. The pellets were then each integrated into short-term storage stock solutions consisting of 1 mL of Phosphate Buffered Saline (PBS) and 50 µL of dimethyl

sulfoxide (DMSO) and vortexed before being stored at 4°C for imminent subsequent usage. The PBS used throughout the entire LIMCALA procedure was standard 1X PBS, with an approximate pH of 7.4, a total phosphate molarity of 11.9 mM, and no chelating agents. A similar short-term stock solution was also created closely preceding the commencement of the LIMCALA workflow with the positive control sample of α-conotoxin VxXXC, which was obtained from CusaBio Technology LLC via their longtime distributor Cosmo Bio USA, Inc. under the product name "Recombinant Conus vexillum Alpha-conotoxin VxXXC". This conotoxin was ordered as a 20 µg lyophilized powder sample. It was stored at -20°C alongside the cryovial venom aliquots before it was used in the LIMCALA procedure for maximum stability and structural preservation.

Conducting LIMCALA

In preparation for the LIMCALA trials, a Horseradish Peroxidase (HRP) detection enzyme solution and a guaiacol detection enzyme-catalyzing reaction buffer were created from HRP and guaiacol lyophilized powders continuously stored at 4°C. The former was composed of HRP dissolved at a concentration of 0.39 mg/mL in PBS. The HRP was obtained from Sigma-Aldrich® and was a Type IV variety with a molar mass of 44,000 kDa. A stock solution composed of guaiacol dissolved at a concentration of 10 mg/mL in DMSO was also prepared. That stock solution was then diluted to 10% concentration in PBS to create a reaction buffer with a final concentration of 1 mg/ml of guaiacol. A blocking buffer solution of PBS with a 5% concentration of Saco Foods® SANALAC Non Fat Dry Milk (NFDM) powder and 125 µL of 0.1 M $Zn(NO_3)_2$ was also created, in addition to a wash buffer solution composed of DI water with a 3% concentration of Sigma-Aldrich®'s TWEEN®-20 biodetergent reagent. Like in the

Enzyme-Linked Immunoabsorbent Assay (ELISA) procedures by which LIMCALA was inspired, the blocking buffer serves to prevent non-specific binding of assay reagents and analytes from binding to the surfaces of the reaction environment container[3]. In LIMCALA workflows, however, the blocking buffer also serves as a chelation buffer that contains Zn^{2+} ions used in the assay's chelate labelling of Cys residues. To begin the assay procedure, each post-freezing, short-term incubated venomic stock solution was diluted in Carbonate-Bicarbonate Buffer to a concentration of 10 µg/mL, forming the coating buffer. 1 mL of that coating buffer solution was applied to the sides of each species venom analyte cuvette. The Carbonate-Bicarbonate buffer was pre-prepared in the laboratory to a total concentration of 50 mM carbonate species in DI water, with 35 mM $NaHCO_3$, 15 mM Na_2CO_3, and a pH of 9.6. The coating buffer, like in both ELISA and IMCAC procedures, served to firmly and securely affix the sample proteins to the walls of the cuvettes. After being removed from the incubator once 12 hours had passed, excess pooled coating buffer was decanted and discarded via pipette. The insides of the cuvettes were then washed via continuous dilution with DI water using 1 mL of the wash buffer.

Following each wash buffer usage, the cuvettes were incubated at 4ºC for exactly 12 hours to allow for the subsequent reagent reactions to be carried out across separate days of laboratory work. However, unexpectedly, these incubation periods without any liquid buffer filling the cuvettes and their reagents adhered to their sides in a condensed film, creating reduction conditions. Such reduction conditions, luckily, served to linearize the normally circular control conotoxin sample and any other whelk or murex protein with conotoxin-like circular

[3] A l mL plexiglass cuvette was used for every experimental and control group analyte.

secondary structures. After the first post-wash 4ºC incubation, 1 mL of the blocking buffer was added to each cuvette and incubated to allow it to function properly for exactly 6 hours at 20°C. The cuvettes were then rinsed with the wash buffer, their liquid contents decanted, and incubated at 4ºC for 12 hours once again. After the second reductive overnight incubation, 1 mL of HRP solution was added to the cuvettes, which were then each incubated at 20°C for 30 minutes in the dark environment of the incubator's interior. Subsequently, the cuvettes underwent a third and final treatment with the wash buffer and overnight incubation under reduction conditions. Finally, 1 mL of reaction buffer was added to each cuvette, followed by 25 µL of a 3% aqueous solution of H_2O_2, a required reactant for any HRP-guaiacol oxidation reaction. The cuvettes were then immediately incubated for 15 minutes at 20°C before being individually stopped using 25 µL of 2 N standard monoprotic HCl, which quickly denatured the HRP reaction by dropping the pH in the cuvette to around 1.4. These stopped reactions were analyzed using the GOYOJO 721 Portable Spectrophotometer, a machine designed for standard UVA-Vis-NIR spectroscopy within the photon wavelength range of 350-1020 nm. For these spectral analyses, a standard solid 1 cm^3 black box-shaped cuvette was used for calibration of the machine.

The negative control cuvette served to provide spectral data to cancel out any noise from the amplified resonance features of the blocking buffer's bovine milk proteins, like casein, which may have otherwise introduced error. For that cuvette, the assay procedure was completed in its entirety except without any venomic analyte component added into the coating buffer. In the positive control cuvette, the coating buffer did not contain any venom obtained from the whelk or murex individuals. Instead, the buffer was formed with the CusaBio 20 µg of α-conotoxin VxXXC lyophilized powder diluted to the same venom concentration of 10 µg/mL as the experimental analyte cuvettes.

Design and Deployment of the LNVSI Algorithm

The LNVSI algorithm is a small, modular, and multivariate Sequential Analysis Pipeline (SAP) and classical machine learning (ML) algorithm written in Python. Microsoft Visual Studio Code's intra-workspace GitHub Copilot (mostly with Anthropic's Claude models) assisted with some debugging, frontend, documentation (namely as some sections of the repository README.md file) , and code cohesivity during development. No artificial intelligence was used for designing the mathematics, pipeline workflow, or conceptual aspects of the algorithm. The algorithm runs several Scikit-learn (sklearn) statistical tests across the UV-Vis-NIR spectrophotometer dataset for each Neogastropod venomic sample cuvette. These computations compare the experimental datasets against the known conotoxin positive control dataset. These tests are classical vector computation, regression, and dimensionality reduction-based[4] ML implementations that serve to determine whether any of the analyte samples are quantitatively conotoxin-like. To that end, following the subtraction of the y-axis absorbance datapoint values of the negative control group from every corresponding datapoint along the x-axis[5] in every relevant dataset, they compare such spectral resonance datasets of the analytes to the positive control dataset. These absorbance datasets are stored as one-dimensional vector arrays, and the comparison logic between the positive control and each analyte always occurs using tuples consisting of those two absorbance arrays paired along the same x-axis wavelength data.

However, before any sklearn ML logic can be called in the algorithm, the aforementioned arrays are preprocessed rigorously. The LNVSI algorithm runs, for each of them, Savitsky-Golay

[4] Mathematical dimensionality reduction, not chemical redox reduction.
[5] Each dataset x-axis consists of wavelength values measured in nanometers

filtering with Bayesian-optimized polynomial orders and window sizes contextual to each smoothed datapoint. The Savitsky-Golay filtering logic also takes a hardcoded bias factor value of 1.2. This preprocessing is done for data normalization and the removal of dataset artifacts that could create errors during downstream ML computation, such as machine imprecision and noise. The smoothed datasets are then automatically saved to the user's device in CSV format. To preface the ML pipeline, the algorithm uses the lmfit algorithm to deconvolve the dataset curves using the Voigt Model alongside a Nonlinear Least Squares regression (Newville et al., 2025). After spectral deconvolution, Dynamic Time Warping (DTW) is applied to align the peak-related data in each tuple to common positions along the shared x-axis. This alignment ensures that spectral resonance features are compared based on their prominence, rather than their exact location on the x-axis. By doing so, DTW improves the accuracy of feature comparison, focusing on the mathematical intensity and shape of the spectral features rather than their precise wavelength positions.

The actual sklearn computations consist of Pearson Correlation Coefficient (PCC) computation, Principal Component Analysis (PCA), an intelligent Partial Least Squares (PLS) regression, and Cosine Similarity Vector Analysis (CSVA). The sklearn.Preprocessing StandardScaler library is also used to further normalize the analyte and positive control tuples mid-pipeline before running PCA for better results accuracy. Once all ML logic has been run on the tuples, the sub-results from each step in the SAP are combined into a Venomic Composite Similarity Score (VCSS) between each analyte venomic peptidome and the positive control. This score is calculated by averaging six normalized metrics: cosine similarity, Pearson correlation, Inverse Euclidean Distance (IED), normalized AUC difference, normalized PCA component difference, and PLS regression score. The IED value for each array tuple is computed between

the processed control and sample curves, then normalized as detailed below to ensure that smaller distances yield higher similarity.

Let:

- P = positive control absorbance curve
- S = sample absorbance curve
- The subscript 2 refers to the Euclidean norm (also called the L2 norm)

$$(\frac{1}{1+|P-S|_2})$$

The full final formula for determining the VCSS is, with “clip” referring to a NumPy function that restricts a value to be never less than 0 and never greater than 1:

$$\text{VCSS} = 100 \times \text{clip}\left(\frac{1}{6}\sum_{i=1}^{6} m_i, 0, 1\right)$$

Where:

- $m_1 = \text{CSVA}(C, S)$

  CSVA result between control (C) and sample (S)

- $m_2 = \frac{\mathrm{PCC}(C, S) + 1}{2}$

  PCC, normalized specifically to [0, 1]

- $m_3 = \frac{1}{1 + |C - S|_2}$

  Inverse Euclidean distance (L2 norm) between control and sample

- $m_4 = 1 - \frac{|\mathrm{AUC}(C) - \mathrm{AUC}(S)|}{\mathrm{AUC}(C)}$

  Normalized difference in AUC

- $m_5 = 1 - |\mathrm{PCA}_1(C) - \mathrm{PCA}_1(S)|$

  Difference in first PCA values represented as subscript 1, normalized.

- $m_6 = \max(\mathrm{PLS}(C, S), 0)$

  PLS regression score, clipped at zero

The composite score quantifies the overall similarity between the sample and control spectra, with the Euclidean distance directly contributing as one of its six core metrics.

Next, the datasets are run through a custom permutation test function. Its logic first calculates the observed composite similarity score VCSS between the control and sample curves, using six metrics, including Euclidean distance. The function is specifically designed for similarity significance testing, avoiding any possible issues that could arise from using a statistical significance test designed for testing for significant divergence patterns as opposed to convergence patterns in scientific data. Next, the sample curve is randomly permuted a large

number of times, represented below using the variable P as n_{P}. For each permutation, P, from the number of permutations, n_{P}, a new permutation similarity score, given by the variable PSS, is computed using the same formula. The test then counts the number of permutations where $\mathrm{PSS} \geq \mathrm{VCSS}$. The final p-value for the tuple in question is finally determined as the fraction of such permutations, given by the equation below:

$$p = \frac{\mathrm{count} + 1}{n_{\mathrm{P}} + 1}$$

After p-values are obtained for each post-analysis tuple[6], False Discovery Rate (FDR) correction using the Benjamini-Hochberg Procedure (BHP) is applied to account for multiple comparisons. This BHP adjustment ensures that the expected proportion of false positives among the analytes deemed significant remains below the hardcoded threshold, based on the standard statistical threshold for statistical significance in science and mathematics of $p < 0.05$. The original spectrophotometer readout is available upon request via email.

The Chemistry of the Spectral Features in LIMCALA

LIMCALA depends on the chemical amplification of spectral resonance features related to the Cys complexes in an analyzed peptidome to allow for its associated spectrophotometer readouts to contain meaningful chemoinformatics data. Software like the LNVSI algorithm simply uses that data, once preprocessed and adjusted using DTW, to compare two different types of venomic peptides between species or taxa. The features amplified include the signatures of HRP/guaiacol oxidation reactions in the Vis region, labile polydentate complexes between the

[6] Each analyte and the positive control dataset it is compared to forms a tuple.

Zn cations and adjacent Cys complexes in the UVA region, and the amide backbones of the analyzed peptides (or whole peptidome) in a sample in the NIR region.

LIMCALA creates conditions where:

- $\mathrm{pH} \approx 1.4$ (after the reaction is stopped using 2N HCl)

- The $\mathrm{SH} \cdots \mathrm{Zn}^{2+}$ complexes are dative-labile dentate complexes, with a monodentate configuration for Zn^{2+} cations associating with single Cys, a bidentate configuration for those associating with adjacent Cys complexes containing two Cys, and, in theoretically uncommon scenarios, a tridentate configuration for those associating with adjacent Cys complexes containing three cysteines.

- The Cys residues' R groups, which are normally thiols, have already been protonated into SH molecules via the post-wash reduction environments and bonded with the Zn^{2+} cations before the HCl dropped the pH. This chemical regime ensures the resilience of the labile dentates even during the final, highly acidic conditions of the cuvettes.

- Since zinc can and does bond with HRP, singular HRP enzymes, while impossible to be exploited to single out individual cysteines, are used to colorimetrically "mark" individual complexes of adjacent or solitary cysteines by amplifying their zinc dentate's signature as a whole.

Given such a chemical situation at the end of a LIMCALA procedure, information on the amount of Cys complexes in a peptide or peptidome can easily be obtained via spectral analysis of the Vis region, where HRP's Soret Band is highly distinct after being oxidized in a guaiacol

reaction. HRP itself is also visually useful for confirming that the "chain" of SH, zinc, and HRP/guaiacol is successfully constructed before the stoppage of the reaction. Such is the case since, due to the vigorous washing of the cuvettes with the wash buffer to remove any excess, nonspecifically bonded, or free zinc cations and HRP enzymes at the appropriate steps, that "chain" must be intact while the reaction is being initiated using H_2O_2. If the entirety of it is not chemically intact, the guaiacol oxidation color change observed in the cuvette will either be nonexistent or very faint. Additionally, it is important to note that, for the bonding of the zinc to the HRP enzymes, the concentration used in LIMCALA is not enough to affect the behavior of the HRP enzymes (Moyo, 2014). The feature's spectral peak, which is owed to the resonance of the tetraguiacol product of the oxidation of the enzyme, is located at 470nm (Koduri & Tien, 1995).

The UVA region of a post-LIMCALA spectrophotometer readout is used to obtain information about the full amount of Cys in a peptide or peptidome and the types of linearly adjacent Cys complexes from the spectral resonance of the actual labile zinc polydentate configuration. Such is the case due to the tendency of metal-thiol dentates to produce, albeit more faintly than at shorter ultraviolet wavelengths, peaks in this region. While other amino acid side chains can form dentate complexes with zinc, these lack, simply based on electronegativity dynamics, the strength of even a protonated thiol's labile bond to a zinc cation. Therefore, they can neither withstand the final drop in pH and potential chelation from free chlorides that come with the addition of HCl at the end of the assay, nor reliably coordinate HRP to produce meaningful resonance data. The same is true for peptide termini that bond with zinc, but they also lack the polyhedral metal-bonding geometry necessary to form true dentates at all.

These polyhedral Cys–Zn dentates are given by peaks observed near 358 nm and 435 nm, for monodentate “C” and bidentate “CC,” respectively. Although those wavelengths correspond to Cys → Cu(II) ligand-to-metal charge-transfer (LMCT) transitions in the cited literature, similar resonance peaks arise in smoothed and unprocessed LIMCALA spectra, even though the metal present is Zn(II) (Brines et al., 2007; Plyusnin et al., 2014). This can be explained by the reduction-based disulfide cleavage in the assay, which converts cystine disulfides (R–S–S$^-$) to protonated thiol (–SH) groups that coordinate Zn^{2+}as dative, labile dentate complexes. This transient coordination occurs because the borderline-acidic zinc ion forms a covalent dative bond with the polarizable, soft-basic thiol group, resulting in a thermodynamically favorable yet kinetically fluid complex that lacks crystal field stabilization energy penalties during ligand exchange. Upon protonation (S$^-$ ⟶ SH), the sulfur’s donor orbital still dominates the transition energy, but its electron-donating power decreases, increasing polarizability and allowing pseudo-LMCT transitions between Sulfur 3p orbitals and empty Zn 4s/4p hybrids. Because these transitions depend mainly on the sulfur donor orbital rather than the specific metal d-manifold, their energy gap remains comparable to that of the Cu(II) LMCT, producing absorption maxima in the same spectral region. In addition, Zn(II)–thiol coordination geometries—typically tetrahedral or distorted polyhedral—preserve S–Zn distances and overlap pathways similar to those in Cu(II) complexes, and the lability of the dentate structure allows dynamic averaging of the coordination environment, broadening and slightly red-shifting the peaks. The resulting spectra

thus display weak, composite envelopes centered near 358 nm and 435 nm, consistent with the polarization-coupled or pseudo-LMCT transitions of Cys(SH)–Zn complexes that mimic Cu(II) LMCT profiles (Vogler & Türk, 1992; Drozd et al., 2018; Matsunaga et al., 2006; Lüdtke et al., 2022).

As for the NIR region, that part of the spectrum is used to get a larger “profile” of the peptide or peptidome’s amide-carboxyl “backbone” and its distinct chemo-organic resonance features. Such organic features, especially important for comparative analysis of Neogastropod myotoxins, are primary amines (the NH_2 N-terminus of a peptide), unbonded carboxyl groups (the $COOH^-$ C-term of a peptide), and primary amides (the $CONH_2$ amidated C-term of a peptide). They are, respectively, best represented by NIR overtone peaks at 779 nm, 1000 nm, and 982 nm, where the NH_2 peak is a doublet, and the $CONH_2$ peak is the average, with the same resulting value for the median and mean, of the appearance range described in the literature of 975-989 nm (Weyer & Lo, 2006).

For spectral deconvolution, the LNVSI algorithm centers entirely around these relevant chemical features of a peptidome spectrophotometric dataplot. This mathematical paradigm is achieved by defining each peak as a center and manually focusing deconvolution to amplify the shape of the dataplot within a ± 30 nm window. The deconvolution logic also took an alpha blend value of 0.8, a σ minimum enforced value of 0.9, and a Γ minimum enforced value of 0.9 as well. In that manner, downstream ML-based analysis and statistical tests were ensured to be fully predicated on the actual chemical features of LIMCALA spectrophotometric readouts. These hardcoded values are then used to systematically prevent the amplification of insignificant noise near feature peaks during deconvolution by setting dynamic upper and lower bounds for

amplification of resonance shapes and peaks on the datasets. Broader, more clearly natural peaks are favored, while tiny peaks are algorithmically suppressed. These tiny peaks could be the result of noise, instrumental error, or insignificant smoothing artifacts, so they are not deconvolved at anywhere near the amplification scale of their broader and more prominent counterparts.

RESULTS

Figure 2

Analyte	Conotoxin-like	Similarity (%)	p-value
Pear Whelk	Yes	86.2186	0.000999001
Apple Murex	Yes	81.6568	0.000999001
Lightning Whelk	Yes	64.6564	0.000999001

The table shows the results of the LNVSI algorithm for the Pear Whelk, Apple Murex, and Lightning Whelk salivary venom samples. Their composite similarity percentages are shown in numerical order from highest to lowest, top to bottom. The analytes were compared to an a-conotoxin VxXXC positive control.

DISCUSSION

The results from this analysis show that all three analytes are quantitatively conotoxin-like based on their very low permutation p-values. The Pear Whelk venomic peptidome showed the highest similarity and, interestingly, stood out as the most conotoxin-like of the three, with the highest VCSS percentage. The Apple Murex sample had strong similarity, yet a slightly lower VCSS than that of the Pear Whelk. The Lightning Whelk sample had a much lower VCSS, but its peptidome, concerning cysteine features, was still statistically significantly similar to α-conotoxin VxXXC's LIMCALA results dataset. Additionally, at the start of these "maiden experiments" with the novel LIMCALA procedure, it was postulated that because muricoideans are phylogenetically closer to conoideans than buccinoideans, the venom of the Apple Murex will be more likely to have a more pronounced presence of peptides with primary structures similar to those of α-conotoxins in its proteome. These hypotheses proved inaccurate in the analysis of the data, given the Apple Murex sample's VCSS value being located numerically between such results from the other two buccinoidean whelk venomic peptidome samples. Such discrepancy in VCSS scores for the Pear Whelk analyte could have been due to unforeseen unique captivity-influenced feeding behaviors, such as an unexpected venomic profile response to Northern Quahog meat.

As for the merits of LIMCALA itself, the framework offers a pragmatic and cost-effective solution for Neogastropod venomic peptidome analysis. HPLC-MS analysis can be quite expensive and hard to access. Thus, it could be helpful to many researchers to use LIMCALA with the LNVSI algorithm or potential future software to come as an intermediary on their proteomic exploration journey for an understudied taxon. However, it is recommended that

future LIMCALA procedures should use Dithiothreitol (DTT) instead of relying on a post-wash condensed film incubation environment for the reduction of the venom proteins. Using DTT would make LIMCALA results more accurate and reproducible. Following the complete removal of all wash buffer liquid, post-wash samples should be filled with a "storage buffer" consisting of 5 mM DTT in 1X PBS. Such a solution contains the recommended concentration of DTT for cleaving the disulfide bonds into –SH Cys side chains, which linearizes circular myotoxins like those found in Neogastropod venom. That concentration simultaneously does not cause denaturation of the peptides (AG Scientific, 2019). Future research on this assay could give rise to more powerful ML and Artificial Intelligence (AI) algorithms and models that could make meaningful bioinformatics conclusions from LIMCALA spectral datasets. The LNVSI algorithm is available via a GitHub repository of the source code accessible at this link: https://github.com/lukelevensaler/LNVSITool. An accessible frontend was developed for the LNVSI algorithm utilizing the PyQt6 framework in Python, thereby minimizing technical barriers to execution for researcher users.

Due to their significant similarity to bioactive conotoxins, the venomic peptidomes of these three species offer promising applications. They represent valuable new frontiers for pharmacology research, cancer treatment, and HPLC-MS profiling. These results are highly promising for further inquiry into the actual structural characteristics and novel classifications of the identified buccitoxins and muritoxins. In the future, HPLC-MS fractionation studies should be undertaken for in vivo cancer cell experiments and more detailed amino acid, secondary structure, tertiary structure, and quaternary structure profiling for further comparison to conotoxins. Perhaps, these buccitoxin and muritoxin peptidomes could contain myotoxins significantly similar not just to conotoxins in general but to α-conotoxins specifically, potentially

enabling anticancer properties.

FUNDING AND COMPETING INTEREST STATEMENT

There are no reviewer conflicts or competing interests to declare. The study was through private family funding with no conditions attached.

REFERENCES

Abraham, N., Healy, M., Ragnarsson, L., Brust, A., Alewood, P., & Lewis, R. (2017). Structural mechanisms for α-conotoxin activity at the human α3β4 nicotinic acetylcholine receptor. *Scientific Reports*, *7*. https://doi.org/10.1038/srep45466

AG Scientific. (2019, May). *Dithiothreitol (DTT) applications you must know*. https://agscientific.com/blog/dithiothreitol-dtt-applications.html

Anand, P., Grigoryan, A., Bhuiyan, M., Ueberheide, B., Russell, V., Quiñonez, J., Moy, P., Chait, B., Poget, S., & Holford, M. (2014). Sample limited characterization of a novel disulfide-rich venom peptide toxin from terebrid marine snail terebra variegata. *PLOS ONE*, *9*, e94122. https://doi.org/10.1371/journal.pone.0094122

Barco, A., Claremont, M., Reid, D., Houart, R., Bouchet, P., Williams, S., Cruaud, C., Couloux, A., & Oliverio, M. (2010). A molecular phylogenetic framework for the Muricidae, a diverse family of carnivorous gastropods. *Molecular Phylogenetics and Evolution*, *56*, 1025–1039. https://doi.org/10.1016/j.ympev.2010.03.008

Bjorn-Yoshimoto, W., Ramiro, I. B., Yandell, M., McIntosh, J., Balmodero, O., Ellgaard, L., & Safavi-Hemami, H. (2020). Curses or cures: A review of the numerous benefits versus the biosecurity concerns of conotoxin research. *Biomedicines*, *8*. https://doi.org/10.3390/biomedicines8080235

Brines, L. M., Shearer, J., Fender, J. K., Schweitzer, D., Shoner, S. C., Barnhart, D., Kaminsky, W., Lovell, S., & Kovacs, J. A. (2007). Periodic trends within a series of five-coordinate thiolate-ligated $[M^{II}(S^{Me2}N_4(tren))]^+$ (M = Mn, Fe, Co, Ni, Cu, Zn) complexes, including a rare example of a stable Cu^{II}–thiolate. *Inorganic Chemistry*, *46*(22), 9267--9277. https://doi.org/10.1021/ic701433p

Buczek, O., Bulaj, G., & Olivera, B. M. (2005). Conotoxins and the posttranslational modification of secreted gene products. *Cellular and Molecular Life Sciences*, *62*, 3067–3079. https://doi.org/10.1007/s00018-005-5283-0

Cruz, L., Gray, W., & Olivera, B. (1978). Purification and properties of a myotoxin from {conus geographus} venom. *Archives of Biochemistry and Biophysics*, *190*, 539–548. https://doi.org/10.1016/0003-9861(78)90308-9

Cunha, R., Lima, F., Tenorio, M., Ramos, A., Castilho, R., & Williams, S. (2014). Evolution at a different pace: Distinctive phylogenetic patterns of cone snails from two ancient oceanic archipelagos. *Systematic Biology*, *63*, 971–987. https://doi.org/10.1093/sysbio/syu059

Drozd, A., Wojewska, D., Peris-Díaz, M. D., Jakimowicz, P., & Krężel, A. (2018). Crosstalk of the structural and zinc buffering properties of mammalian metallothionein-2. *Metallomics*, *10*(4), 595–613. https://doi.org/10.1039/c7mt00332c

Fedosov, A., Puillandre, N., Herrmann, M., Dgebuadze, P., & Bouchet, P. (2017). Phylogeny, systematics, and evolution of the family Costellariidae (Gastropoda: Neogastropoda). *Zoological Journal of the Linnean Society*, *179*. https://doi.org/10.1111/zoj.12431

Fedosov, A., Zaharias, P., Lemarcis, T., Modica, M. V., Holford, M., Oliverio, M., Kantor, Y., & Puillandre, N. (2024). Phylogenomics of Neogastropoda: The backbone hidden in the bush. *Systematic Biology*, *73*. https://doi.org/10.1093/sysbio/syae010

Flinn, J., Pallaghy, P., Lew, M., Murphy, R., Angus, J., & Norton, R. (1999). Role of disulfide bridges in the folding, structure and biological activity of ω-conotoxin GVIA. *Biochimica et Biophysica Acta (BBA) - Protein Structure and Molecular Enzymology*, *1434*, 177–190. https://doi.org/10.1016/s0167-4838(99)00165-x

Gao, B., Peng, C., Yang, J., Yi, Y., Zhang, J., & Shi, Q. (2017). Cone snails: A big store of conotoxins for novel drug discovery. *Toxins*, *9*(12), 397. https://doi.org/10.3390/toxins9120397

Gencic, S., LeClerc, G. M., Gorlatova, N., Peariso, K., Penner-Hahn, J. E., & Grahame, D. A. (2001). Zinc--thiolate intermediate in catalysis of methyl group transfer in {methanosarcina barkeri}. *Biochemistry*, *40*(43), 13068–13078. https://doi.org/10.1021/bi0112917

Gorson, J., Ramrattan, G., Verdes, A., Wright, E., Kantor, Y., Srinivasan, R. R., Musunuri, R., Packer, D., Albano, G., Qiu, W.-G., & Holford, M. (2015). Molecular diversity and gene evolution of the venom arsenal of terebridae predatory marine snails. *Genome Biology and Evolution*, *7*, 1761–1778. https://doi.org/10.1093/gbe/evv104

Heller, J. (2015). *Predators*. Springer Nature. https://doi.org/10.1007/978-3-319-15452-7

Hernández-Sámano, A., Falcón, A., Zamudio, F., Ortíz-Arellano, M., López-Vera, E., & Aguilar, M. (2020). A turripeptide from {polystira nobilis} venom inhibits human α3β2 and α7 nicotinic acetylcholine receptors. *Insect Biochemistry and Molecular Biology*, *124*, 103416. https://doi.org/10.1016/j.ibmb.2020.103416

Human. (1999). *Marine-derived pharmaceuticals and related bioactive agents* (pp. 73–82). National Academies Press. https://www.ncbi.nlm.nih.gov/books/NBK230696/

Imperial, J., Kantor, Y. I., Watkins, M., Heralde, F., Stevenson, B., Chen, P., Hansson, K., Stenflo, J., Ownby, J.-P., Bouchet, P., & Olivera, B. (2007). Venomous auger snail Hastula (Impages) hectica (Linnaeus, 1758): molecular phylogeny, foregut anatomy and comparative toxinology. *Journal of Experimental Zoology Part B: Molecular and Developmental Evolution*, *308B*(6), 744–756. https://doi.org/10.1002/jez.b.21195

Kendel, Y., Melaun, C., Kurz, A., Nicke, A., Peigneur, S., Tytgat, J., Wunder, C., Mebs, D., & Kauferstein, S. (2013). Venomous secretions from marine snails of the terebridae family target acetylcholine receptors. *Toxins*, *5*, 1043–1050. https://doi.org/10.3390/toxins5051043

Krizek, B. A., Merkle, D. L., & Berg, J. M. (1993). Ligand variation and metal ion binding specificity in zinc finger peptides. *Inorganic Chemistry*, *32*(6), 937–940. https://doi.org/10.1021/ic00058a030

Kuznetsova, K., Zvonareva, S., Ziganshin, R., Mekhova, E., Dgebuadze, P., Yen, T., Nguyen, T., Moshkovskii, S., & Fedosov, A. (2022). Vexitoxins: Conotoxin-like venom peptides from predatory gastropods of the genus Vexillum. *Proceedings of the Royal Society of Biological Sciences*, *289*(1980). https://doi.org/10.1098/rspb.2022.1152

Li, R., Bekaert, M., Wu, L., Mu, C., Song, W., Migaud, H., & Wang, C. (2019). Transcriptomic analysis of marine gastropod hemifusus tuba provides novel insights into conotoxin genes. *Marine Drugs*, *17*(8), 466. https://doi.org/10.3390/md17080466

Li, X., Chen, W., Zhangsun, D., & Luo, S. (2020). Diversity of conopeptides and their precursor genes of conus litteratus. *Marine Drugs*, *18*, 464. https://doi.org/10.3390/md18090464

Lüdtke, N., Kuhnt, J., Heil, T., Steffen, A., & Marian, C. M. (2022). Revisiting ligand-to-ligand charge transfer phosphorescence emission from zinc(II) diimine bis-thiolate complexes: It is actually thermally activated delayed fluorescence. *ChemPhotoChem*, *7*(1). https://doi.org/10.1002/cptc.202200142

Matsunaga, Y., Fujisawa, K., Ibi, N., Fujita, M., Ohashi, T., Amir, N., Miyashita, Y., Aika, K., Izumi, Y., & Okamoto, K. (2006). Sulfur K-edge extended x-ray absorption fine structure spectroscopy of homoleptic thiolato complexes with zn(II) and CD(II). *Journal of Inorganic Biochemistry*, *100*(2), 239--249. https://doi.org/10.1016/j.jinorgbio.2005.11.004

Moyo, M. (2014). Horseradish peroxidase biosensor to detect zinc ions in aqueous solutions. *Open Journal of Applied Biosensor*, *03*(01), 1–7. https://doi.org/10.4236/ojab.2014.31001

Möller, C., Davis, W., Clark, E., DeCaprio, A., & Marí, F. (2019). {Conodipine-P1-3}, the first phospholipases {a2} characterized from injected cone snail venom. *Molecular & Cellular Proteomics*, *18*(5), 876a--891. https://doi.org/10.1074/mcp.ra118.000972

Newville, M., Otten, R., Nelson, A., Stensitzki, T., Ingargiola, A., Allan, D., Fox, A., Carter, F., & Rawlik, M. (2025). *LMFIT: Non-linear least-squares minimization and curve-fitting for python*.

Osipov, A., Terpinskaya, T., Yanchanka, T., Balashevich, T., Zhmak, M., Tsetlin, V., & Utkin, Y. (2020). A-conotoxins enhance both the in vivo suppression of Ehrlich

carcinoma growth and in vitro reduction in cell viability elicited by cyclooxygenase and lipoxygenase inhibitors. *Marine Drugs*, *18*(4), 193. https://doi.org/10.3390/md18040193

Peng, C., Tang, S., Pi, C., Liu, J., Wang, F., Wang, L., Zhou, W., & Xu, A. (2006). Discovery of a novel class of conotoxin from conus litteratus, LT14A, with a unique cysteine pattern. *Peptides*, *27*, 2174--2181. https://doi.org/10.1016/j.peptides.2006.04.016

Plyusnin, V., Pozdnyakov, I., Grivin, V., Solovyev, A., Lemmetyinen, H., Tkachenko, N., & Larionov, S. (2014). Femtosecond spectroscopy of the dithiolate Cu(II) and Ni(II) complexes. *Dalton Transactions*, *43*(47), 17766–17774. https://doi.org/10.1039/c4dt01407c

Ringeval, A., Modica, M. V., Kantor, Y., Tenorio, M. J., Galindo, J. C. G., Puillandre, N., & Farhat, S. (2026). Multi-omics characterization of toxin expression and producing organs in the predatory gastropods monoplex corrugatus and Stramonita Haemastoma. *BMC Genomics*, *27*(1). https://doi.org/10.1186/s12864-026-12592-3

Robinson, S., & Norton, R. (2014). Conotoxin gene superfamilies. *Marine Drugs*, *12*, 6058–6101. https://doi.org/10.3390/md12126058

Safavi-Hemami, H., Brogan, S., & Olivera, B. (2019). Pain therapeutics from cone snail venoms: From {ziconotide} to novel non-opioid pathways. *Journal of Proteomics*, *190*, 12–20. https://doi.org/10.1016/j.jprot.2018.05.009

Song, H., Yu, Z.-L., Sun, L.-N., Xue, D.-X., Zhang, T., & Wang, H.-Y. (2016). Transcriptomic analysis of differentially expressed genes during larval development of rapana venosa by digital gene expression profiling. *G3 Genes|Genomes|Genetics*, *6*(7), 2181–2193. https://doi.org/10.1534/g3.116.029314

Türk, T., Resch, U., Fox, M. A., & Vogler, A. (1991). *Spectroscopic studies of zinc benzenethiolate complexes: Electron transfer to methyl viologen*. Regensburg University. https://epub.uni-regensburg.de/13366/1/vogler65.pdf

Urani, A., Romieu, P., Portales-Casamar, E., Roman, F., & Maurice, T. (2002). The antidepressant-like effect induced by the SIGMA1 (σ1) receptor agonist igmesine involves modulation of intracellular calcium mobilization. *Psychopharmacology*, *163*, 26–35. https://doi.org/10.1007/s00213-002-1150-y

Vaux, F., Hills, S., Marshall, B., Trewick, S., & Morgan-Richards, M. (2017). A phylogeny of Southern Hemisphere whelks (Gastropoda: Buccinulidae) and concordance with the fossil record. *Molecular Phylogenetics and Evolution*, *114*, 367--381. https://doi.org/10.1016/j.ympev.2017.06.018

Weyer, L., & Lo, S.-C. (2006). Spectra-structure correlations in the near-infrared. In *Handbook of Vibrational Spectroscopy*. https://doi.org/10.1002/9780470027325.s4102

Xu, P., Xiong, Y., Liu, Y., Yu, S., Zhangsun, D., Wu, Y., & Luo, S. (2019). Degradation kinetics of α-conotoxin TxID. *FEBS Open Bio*, *9*, 1561–1572. https://doi.org/10.1002/2211-5463.12697

Supplementary Files

This is a list of supplementary files associated with this preprint. Click to download.

- alldatapreprocessed.csv